Microchimica Acta (2020) 187:607
https://doi.org/10.1007/s00604-020-04581-4

ORIGINAL PAPER

A novel electrochemical biosensor based on peptidoglycan and platinum-nickel-copper nano-cube for rapid detection of Gram-positive bacteria

Daobin Han[1] · Yurong Yan[1] · Xintong Bian[1] · Jianmin Wang[1] · Min Zhao[1] · Xiaolei Duan[1,2] · Liangsheng Kong[1] · Wei Cheng[3] · Shijia Ding[1]

Received: 3 April 2020 / Accepted: 29 September 2020

Abstract

A novel non-enzyme electrochemical biosensor for the rapid detection of Gram-positive bacteria has been constructed that relys on a stable and efficient combination between the peptidoglycan layer and platinum-nickel-copper nanocubes (Pt-Ni-Cu NCs). Briefly, bacteria were first captured by a specific antibody. Then, the electrochemical signal materials (Pt-Ni-Cu NCs) were bound to the bacteria peptidoglycan layer using specific structural and surface features. The rapid and sensitive bacterial detection was then achieved using intrinsic electrochemical characteristics and superoxidase-like activity of the Pt-Ni-Cu NCs. Moreover, the nature of peptidoglycan covering the whole bacteria provided the premise for signal amplification. Under optimal conditions, the electrochemical signal variation was proportional to the concentration of bacteria ranging from 1.5×10^2 to 1.5×10^8 CFU/mL with a detection limit of 42 CFU/mL using a working potential of − 0.4 V. This electrochemical biosensor has been successfully applied to detect bacteria concentrations in urine samples, and the recoveries range from 90.4 to 107%. The proposed biosensor could be applied for broad-spectrum detection of Gram-positive bacteria since most Gram-positive bacteria possess a thick peptidoglycan layer. The developed electrochemical biosensing strategy might be used as a potential tool for clinical pathogenic bacteria detection and point-of-care testing (POCT).

Keywords Peptidoglycan · Pt-Ni-Cu NCs · Gram-positive bacteria · Electrochemical biosensor

Introduction

The world is on the cusp of a "post-antibiotic era." According to the latest statistics, drug-resistant super-bacteria cause approximately 35,000 deaths each year [1]. Extremely multi-resistant bacteria, such as *Staphylococcus aureus* (*S. aureus*) and *Streptococcus pneumoniae* (*S. pn*), are the major cause of most wide-ranging diseases [2, 3]. In addition, an increasing number of bacterial gene mutations have been detected, which significantly slows down the control of harmful bacteria. Therefore, the development of rapid and sensitive detection methods is essential for the prevention and control of pathogenic bacteria in the environment.

Common bacterial detection methods, such as PCR and ELISA, possess high specificity in clinical detection; yet, those methods are time-consuming, costly, and can generate cross-contamination [4]. Biosensing technologies, such as fluorescence [5], chemiluminescence [6], electrochemical luminescence [7], electrochemistry [8, 9], and surface plasmon resonance [10] can improve detection sensitivity and shorten detection time by exploiting novel signal amplification strategies and nanomaterials. Among them, electrochemical biosensing methods have been widely investigated for the detection of bacteria due to

Daobin Han and Yurong Yan contributed equally to this work.

Electronic supplementary material The online version of this article (https://doi.org/10.1007/s00604-020-04581-4) contains supplementary material, which is available to authorized users.

✉ Shijia Ding
dingshijia@163.com

[1] Key Laboratory of Clinical Laboratory Diagnostics (Ministry of Education), College of Laboratory Medicine, Chongqing Medical University, Chongqing 400016, China

[2] Department of Laboratory Medicine, The Affiliated Hospital of Zunyi Medical University, Zunyi 563000, Guizhou, China

[3] The Center for Clinical Molecular Medical detection, The First Affiliated Hospital of Chongqing Medical University, Chongqing 400016, China

Published online: 14 October 2020

their convenient operation, simple preparation, and high sensitivity [11, 12]. Recently, Ding et al. developed a sensitive electrochemical DNA biosensor for specific detection of *Enterobacteriaceae* by exonuclease III–assisted signal amplification [13]. However, traditional electrochemical biosensing methods require the catalysis of protease with strict control of the temperature and pH of the reaction system, which increases the cost. Thus, researchers are actively seeking stable mimetic enzymes to explore the redox and catalysis characteristics on the electrochemical platform, thus demonstrating potential alternatives for protease.

Over recent years, different kinds of advanced nanomaterials, such as noble metal nanomaterials, metal oxide nanomaterials, carbon nanomaterials, and bio-nanomaterials, have been extensively used in biosensors and diagnostic drugs due to their excellent photocatalytic performance, conductivity, and modifiability [14, 15]. Peroxidase-like materials, such as transition metals and metal-organic frameworks, have an important role in electrochemical biosensing due to their stable and efficient catalytic activity [16, 17]. Particularly, platinum nanoparticles and palladium nanoparticles are the representative nanoparticles of transition metals that are often used as mimetic enzymes in the photoelectrochemical field; they offer high plasticity, easy synthesis, and high catalytic efficiency [18]. Especially, different Pt nanomaterials with different shapes have been found to own enzyme mimetic activities such as peroxidase, catalase superoxide dismutase, and oxidase [19]. More importantly, it has been reported that among pure metals, Pt is the most efficient electrocatalyst [20]. Compared with Au, Ag nanoparticles, the Pt nanoparticles possess high catalytic activity and stability. Furthermore, the stable crystal surfaces and polyhedral nanostructures of Pt nanoparticles with different shapes are easily synthesized, which significantly improve the catalytic efficiency [21]. The small size platinum nanostructures have good biocompatibility in biological studies [22]. Moreover, introducing another metal into Pt to form nano-alloys or nano-composites can enhance catalytic activity and stability of the materials. Hence, Pt was selected as signal materials for electrocatalysis.

Although a single nano-metal catalyst displays certain performance in reactions, there are still some weaknesses that need to be solved, including catalytic activity and structural stability. Moreover, introducing another metal into a single nano-metal catalyst to form nano-alloys or nano-composites is a highly effective way to enhance catalytic activity. Previous studies have provided support for the synergistic effect among metals [23, 24]. For example, an Au@Pd NDs/Fe^{2+}-CS/PPy NT based on sandwich-type amperometric immunosensor was fabricated for sensitive detection of CEA [25]. As transition metals, the nanomaterial of platinum, nickel, and copper possesses high catalytic activity for H_2O_2. Based on the above synergistic theory, the ternary nano-composites of platinum-nickel-copper nanocubes (Pt-Ni-Cu NCs) were firstly applied for bacterial electrochemical biosensing detection by the strong peroxidase-like effect in this work. In addition, both nickel and copper of Pt-Ni-Cu NCs all have intrinsic characteristic oxidation peaks that can be used to build electrochemical biosensor without additional catalysis substance, directly generating electrochemical signals.

Traditional bacterial electrochemical immunosensor output signals use aptamers or antibodies based on the sandwich structure [26]. Modified secondary antibodies are also needed in electrochemical immunosensors, which not only complicate the experiment procedures but also significantly increase the cost of the experiment. Compared with ordinary human cells, bacteria have some unique structures (peptidoglycan, phosphoteichoic acid, capsular polysaccharide, etc.), which are stable in bacterial inheritance [27]. These structures have been extensively researched in the pathogenesis of bacteria, but few developments on bacterial biosensors have been reported so far [28]. The special spatial configuration and biological characteristics of these structures can greatly enhance the specificity and sensitivity of bacterial detection. Furthermore, the combination of special structures and nanomaterials makes bacterial detection and antibacterial treatments easier and more effective. For example, spines and polyhedral nanomaterials can penetrate the tight membranous of Gram-negative bacteria [29]. Yet, compared with Gram-negative microorganisms, Gram-positive bacteria have a thicker peptidoglycan network on the outer layer of bacteria. Their peptidoglycan possesses a multilayer network macromolecule structure, formed by the polymerization of acetylglucosamine [30, 31], acetylmuric acid, and four to five amino acid short peptides [32], with the maximum thickness up to 50 nm. Moreover, the peptidoglycan has some viscosity, which can be easily combined with a nano-plane [33]. Opportunely, nanocubes possess a large, uniform, and horizontal surface [34], which can easily attach to the peptidoglycan layer and stay in the peptidoglycan to provide the antibacteria effect through the enzyme-like activities. In this study, the efficient combination effect of Pt-Ni-Cu NCs and peptidoglycan was investigated on the electrochemical biosensor of bacterial detection.

Herein, based on the high peroxidase activity of Pt-Ni-Cu NCs and its efficient combination with peptidoglycan, a non-enzyme electrochemical biosensor was constructed for the rapid detection of Gram-positive bacteria. As shown in Scheme 1, Pt-Ni-Cu NCs were synthesized by three metal substrates using a hydrothermal method in a reactor. Firstly, the C-CNTs were naturally deposited on the electrode surface; this could enhance electron transfer accompanying by increasing the effective reaction area. The following

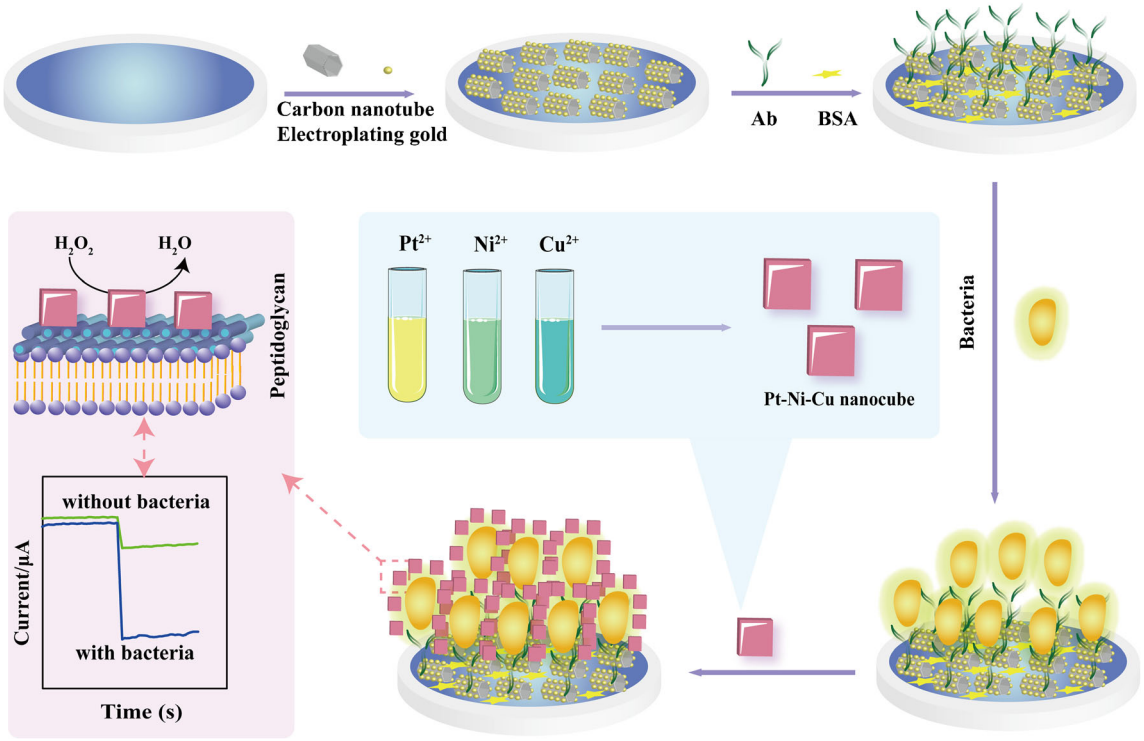

Scheme 1 Schematic illustration of the electrochemical biosensor for Gram-positive bacteria detection

electrodeposition of AuNPs on the C-CNT-modified electrode surface would further increase the conductivity, which had the function of binding with thiol-terminated antibodies. Accordingly, target bacteria were captured explicitly by specific antibodies. Then, Pt-Ni-Cu NCs were firmly combined with the peptidoglycan on the surface of Gram-positive bacteria. Due to their extensive surface coverage of peptidoglycan, each bacterium could bind multiple Pt-Ni-Cu NCs.

Materials and methods

Materials

Carbon nanotubes (CNTs, > 95%), gold chloride ($HAuCl_4$, > 99%), potassium chloroplatinate (K_2PtCl_4, > 99%), nickel chloride hexahydrate ($NiCl_2{\cdot}6H_2O$, > 99%), copper nitrate trihydrate ($Cu(NO_3)_2{\cdot}3H_2O$, 99%), concentrated nitric acid (HNO_3, AR), sulfuric acid (H_2SO_4, AR), hydrogen peroxide (H_2O_2, AR), and bovine serum albumin (BSA, MB grade) were bought from Sigma-Aldrich (USA). Strains of *Escherichia coli* (*E. coli*), *S. au22923*, *S. au21293*, *S. pn*, *Pseudomonas aeruginosa* (*P. ae*), and *Klebsiella pneumonia* (*K. pn*) were provided by the Affiliated Hospital of Zunyi Medical University. Luria-Bertani medium (LB, FMB Grade), Columbia blood plate, polyvinyl pyrrolidone (PVP, MW30000, MB grade), glycine (GLY, MB grade), phosphate buffer solution (PBs, 2.7 mM KCl, 137 mM NaCl, 1.8 mM KH_2PO_4, 8 mM Na_2HPO_4) (MB grade), glycerine (MB grade), and Todd Hewitt broth (THB, FMB Grade) were purchased from Sangon Inc. (Shanghai, China, www.sangon.com). Antibodies of anti-*S. aureus* and anti-*S. pn* were purchased from Biosynthesis Inc. (Beijing, China, www.bioscience-tj.com). All the solutions were prepared using deionized water (≥ 18 MΩ, Milli-Q, Millipore, www.mollipore.com).

Apparatus

The electrochemical detections were carried out by the CHI660D electrochemistry workstation (Chenhua Instruments, China, www.chinstr.com). A three-electrode system consisted of a modified gold electrode (GE, 3 mm) as a working electrode, a platinum wire as a counter electrode, and an Ag/AgCl electrode as a reference electrode. The bacteria were cultured in a USemerfer/Thermo carbon dioxide cell culture chamber (Thermo Fisher, USA, www.thermofisher.com) and Zwdy-240 of full-temperature multi-amplitude orbital shaker (Zhicheng Instruments, China, www.zhicheng-sh.cn). The morphology of the nanomaterials was characterized by H-7500 transmission electron microscopy and SU8000 scanning electron microscopy (SEM) (Hitachi, Japan, www.hitachi-hightech.com). The instrument used for infrared

characterization was Thermo Scientific Nicolet iS50 (Thermo Fisher, USA, www.thermofisher.com).

Bacteria culture

The strains of *E. coli*, *S. aureus*, *P. ae*, and *K. pn* were grown in LB broth medium; *S. pn* was grown in THB medium. All bacteria were grown at 37 °C, with continuous shaking for 8 h. The plate colony counting method was used to count bacteria and adjust colony concentration to 1.5×10^8 CFU/mL. The bacteria were collected in a 1.5-mL Eppendorf tube by centrifuging at 5000 rpm for 5 min and then washing three times by 0.01 M PBs. Finally, the collected bacteria sediments were re-suspended with 0.01 M PBs and applied to the electrochemical biosensor in different concentrations.

Synthesis of C-CNTs

C-CNTs were compounded as previously described [35] with minor modifications. Firstly, 0.5 g CNT powders were added to 60 mL HNO_3, which was oxidized at 100 °C for 12 h. After cooling down to room temperature, the mixed liquids were diluted with 60 mL deionized water and subsequently centrifuged at 15000 rpm for 20 min. Then, the sediments were continuously washed with deionized water until pH turned to neutral and was dried in the oven to obtain a powder. Finally, C-CNTs were successfully prepared and kept in a sealed bottle.

Synthesis of Pt-Ni-Cu NCs

Pt-Ni-Cu NCs were synthesized according to the reported literature [36] with minor modification. Firstly, 2 mL of 0.02 M K_2PtCl_4, 4 mL of 1.66 mM Cu $(NO_3)_2 \cdot 3H_2O$, 4 mL of 1.66 mM $NiCl_2 \cdot 6H_2O$, and 450 mg PVP were added to a beaker by continuously agitating on a magnetic agitator for 10 min. When PVP dissolved completely, 80 mg GLY was added to the above system with another 5 min stirring. Subsequently, the above system was transferred to the ultrasonic instrument for 10 min, and the system was sealed in the reactor. After that, the reactor was put into the oven, heated to 200 °C, and kept for 6 h. Finally, the resulting dark brown products were collected by centrifuging at 9000 rpm for 10 min. The sediments were washed three times using anhydrous ethanol and deionized water in turn to get the pure Pt-Ni-Cu NCs. In the synthesis process, two points that had a close relationship with the plasticity of the Pt-Ni-Cu NCs required special attention. One was the amount of glycine, and the other was that the heating time needed to be calculated from room temperature instead of 200 °C.

Validation of the combination of peptidoglycan and Pt-Ni-Cu NCs

Firstly, a single bacteria colony selected from the blood plate was cultured in a liquid medium. The bacterial solution was incubated at 37 °C in a concentrator with 200 rpm. After reaching bacterial liquid turbidity of 0.5 maxwell, the bacterial concentration was adjusted to 1.5×10^8 CFU/mL. Then, a 200 μL bacterial solution was added to 200 μL Pt-Ni-Cu NC solution, which was incubated with 300 rpm at 37 °C for 1 h. Consequently, the bacteria were washed three times by 0.01 M PBs and mixed with 200 μL glutaraldehyde stationary solution to fix the bacteria. Finally, the fixed bacteria were observed by SEM [33].

Fabrication of electrochemical biosensor

Firstly, the working electrode (GE) was polished by 0.05 μm alumina slurries for 5 min. Next, the GE was treated with piranha solution (H_2SO_4: H_2O_2 = 3:1) for 5 min, which was repeated for 3 times, and was then sonicated in deionized water to obtain a clean electrode. A total of 7 μL C-CNTs (1 mg/mL) were added to the polished GE. When dried, the C-CNT-modified GE was dipped in 1% $HAuCl_4$ solution to obtain an electroplated AuNP layer by deposition potential of − 0.2 V for 30 s. After that, 10 μL of 10 μg/mL antibody for bacteria was added to the AuNP-modified GE, with incubating for 8 h at 4 °C. Subsequently, 8 μL of 0.01 g/mL BSA solution was added to the antibody-modified GE to block the unconjugated place of the AuNPs layer for 0.5 h at 37 °C. Then, the antibody-modified GE was incubated in different concentrations of target bacteria at 37 °C for 80 min. Finally, Pt-Ni-Cu NC solutions were coated onto the modified GE at 37 °C for 60 min [37]. After layer-by-layer modification, an electrochemical biosensor for the detection of Gram-positive bacteria was successfully constructed.

Electrochemical measurement

Cyclic voltammetry (CV) and electrochemical impedance spectroscopy (EIS) detection were implemented in 0.1 M KCl containing 5.0 mM $[Fe(CN)_6]^{3-/4-}$. Five mV of the applied sine wave potential were set in EIS, with the frequency range of 10^{-2}–10^5 Hz and the scanning potential of CV was set from − 0.2 to 0.6 V. The differential pulse voltammetry (DPV) was measured in 0.01 M PBs from 0.075 to 0.35 V. The amperometric i-t curve (i-t) was used to detect the current density characteristics of the electrochemical biosensor. After the background current density was steady, the H_2O_2 was put into 0.01 M PBs to achieve 5 mM of the final concentration under stirring at the working potential − 0.4 V [38].

Results and discussion

Characterization of different nanomaterials

The morphologies of the Pt-Ni-Cu NCs were characterized by TEM, SEM, and energy dispersive spectrometer (EDX), respectively. As shown in Fig. 1a, the Pt-Ni-Cu NCs were uniformly distributed, showing the relatively homogeneous shape and size. Similarly, particles with uniform size and cube-shape were evenly distributed in TEM (Fig. 1b). The cube size was approx. 35 nm. The element composition of Pt-Ni-Cu NCs was further verified in Fig. 1c, which further confirmed the successful synthesis of Pt-Ni-Cu NCs.

In order to improve the solubility of CNTs in aqueous solution and the sensitivity of the electrochemical biosensor, CNTs were modified with carboxyl groups by acid treatment. Figure S1 indicated an infrared absorption peak of carboxyl groups at 1730 cm^{-1} compared with the unmodified CNTs. The carboxyl group absorbed most photons at this wavelength, which was consistent with the previous literature reports [38].

The combination of bacterial peptidoglycan and Pt-Ni-Cu NCs

In order to examine the binding effect of bacteria peptidoglycan with the Pt-Ni-Cu NCs, bacteria were co-cultured with the nanomaterials and consequently washed and immobilized on the sheet copper. The combination products were characterized using SEM, which was the most direct way to evaluate the combination ability. Firstly, the binding efficiency of Gram-positive bacteria (*S. aureus*) to Pt-Ni-Cu NCs was verified. As shown in Fig. 2a, b, Pt-Ni-Cu NCs were uniformly distributed on the surface of *S. aureus*, and the degrees of combination were different. Besides, the size and shape of the cubes did not change. Contrary, no stable binding effect was observed for Gram-negative *E. coli* (Fig. 2c, d), and only a few cubes were distributed in the field of vision. The above results confirmed that the thicker peptidoglycan layer of Gram-positive bacteria may provide higher binds to Pt-Ni-Cu NCs compared with Gram-negative bacteria, which has thinner peptidoglycan layer.

Characterization of the electrochemical biosensor

CV and EIS were used to confirm the layer-by-layer modification on the electrode, respectively. CV was directly determined by the conductivity of the modified materials on the electrode (Fig. 3a). The bare electrode showed good conductivity (curve a). There was a marked increase after modifying C-CNTs (curve b), which indicated that the conductivity of the electrode could be effectively enhanced by the conjugation effect of the C-CNTs. Next, the current was further enhanced with the modification of AuNPs (curve c), because it possessed more free electrons. The current then decreased after modifying with antibody and BSA (curve d and e) in succession, which resulted from the conductivity obstruction of the protein. Finally, the target bacteria (curve f) and Pt-Ni-Cu NCs (curve g) were combined to the electrodes in turn, with a slight decrease of the current. The electrochemical active surface areas of the electrodes were calculated via Randles-Sevcik equation [39] (supporting information). The abundant reaction area and surface free electrons of C-CNTs/AuNPs resulted in good electrical conductivity and ideal electrochemical signal output.

Similarly, the results of EIS (Fig. 3b) were in accordance with CV, which first decreased and then increased, where the radius of the curve represented the resistance. The Randle equivalence circuit that insetted in Fig. 3b consisted of R_{ct}, R_s, W, and C_{dl}, representing charge transfer resistance, solution resistance, Warburg constant, and double layer capacitance, respectively [40]. The results of the CV and EIS fully confirmed the successful layer-by-layer assembly on the electrode surface, and the results provided an essential precondition for subsequent electrochemical signal output.

As already mentioned, Pt-Ni-Cu NCs could be used as peroxidase-like enzymes to produce electrocatalytic signals

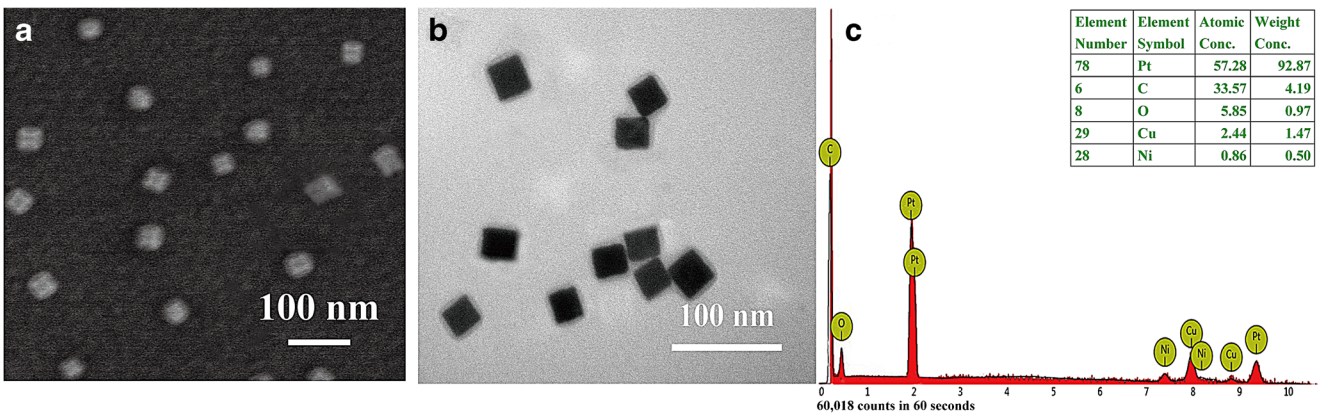

Fig. 1 Characterization of Pt-Ni-Cu NCs. **a** SEM images; **b** TEM images; **c** EDS

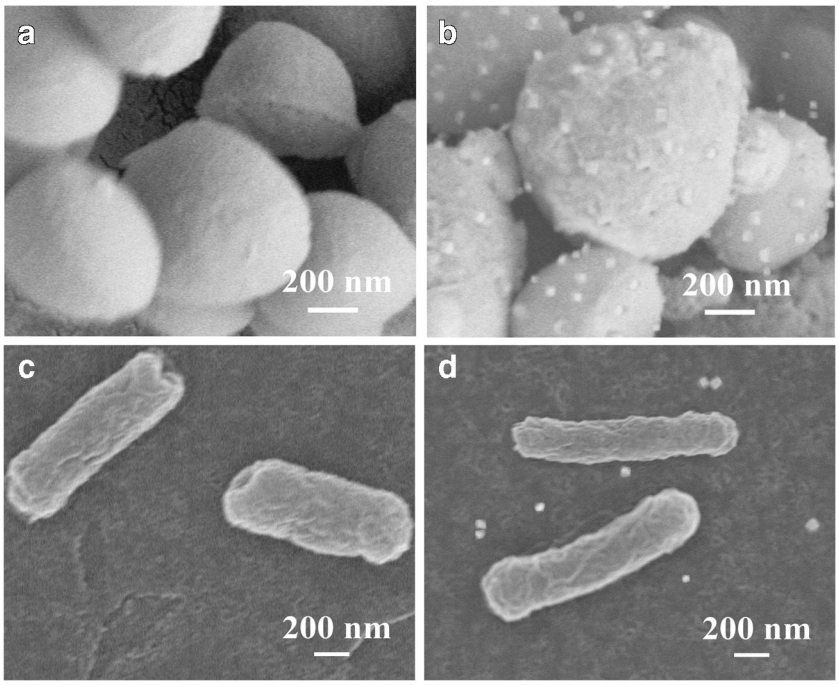

Fig. 2 Binding efficiency of Gram-positive (*S. aureus*) and Gram-negative (*E. coli*) to Pt-Ni-Cu NCs. **a**, **b** The SEM of *S. aureus* mixed with (**b**) or without (**a**) Pt-Ni-Cu NCs. **c**, **d** The SEM of *E. coli* with (**d**) or without (**c**) Pt-Ni-Cu NCs

by efficiently catalyzing H_2O_2. The sensitive method of i-t (Fig. 4a) was used to further characterize the feasibility of the scheme in 0.01 M PBs with H_2O_2. Compared with the other electrochemical methods, i-t had higher sensitivity, which was suitable for the detection of the low concentration target. The current density value at the reduction peak of oxygen was continuously detected with the catalysis effect of Pt-Ni-Cu NCs in the working potential of − 0.4 V. When there were no bacteria, the Pt-Ni-Cu NCs could not combine to the modified electrode, showing a low background signal. In the presence of bacteria, the Pt-Ni-Cu NCs and bacterial peptidoglycan were closely combined. Consequently, the i-t signal was enhanced, increasing the concentration of the target bacteria. Therefore, the results of i-t confirmed the feasibility of the electrochemical biosensor.

Besides, trimetallic Pt-Ni-Cu NCs could output metal oxidation peaks due to the intrinsic electrochemical properties. As shown in Figure S2, the Pt-Ni-Cu NCs had obvious characteristic peaks at about 0.2 V compared with the electrode without it in 0.01 M PBs. Hence, we speculated that this was a self-oxidation peak of copper and nickel, which was first applied to the electrochemical biosensor. Based on the above results, DPV (Fig. 4b) was used to characterize the feasibility, carrying out in 0.01 M PBs. Similar to i-t, when there were no target bacteria, the background signal was low. However, in the presence of bacteria, the DPV signal significantly increased. The signal was further improved with the increase of the target. The DPV results once again confirmed the feasibility of the electrochemical biosensor.

The reaction condition optimization of the electrochemical biosensor

In order to improve the sensitivity of the electrochemical sensor, thus saving time and costs, the key conditions in the experiment were optimized. The signal intensity was directly

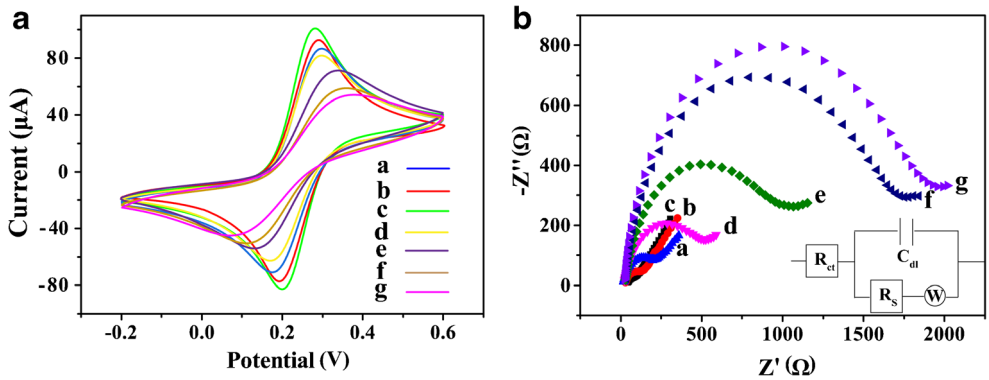

Fig. 3 Characterization of the electrochemical biosensor. CV (**a**) and EIS (**b**) of electrodes with different modifications in solution of 5 mM $Fe(CN)_6^{3-/4-}$ in 0.1 M KCl: a, bare GE: b, C-CNTS/GE: c, AuNPs/C-CNTS/GE: d, Ab/AuNPs/C-CNTS/GE: e, BSA/Ab/AuNPs/C-CNTS/GE: f, *S. aureus*/BSA/Ab/AuNPs /C-CNTS/GE: g, Pt-Ni-Cu NCs/*S. aureus*/BSA/Ab/AuNPs/C-CNTS/GE. Inset of **b** was the equivalent circuit

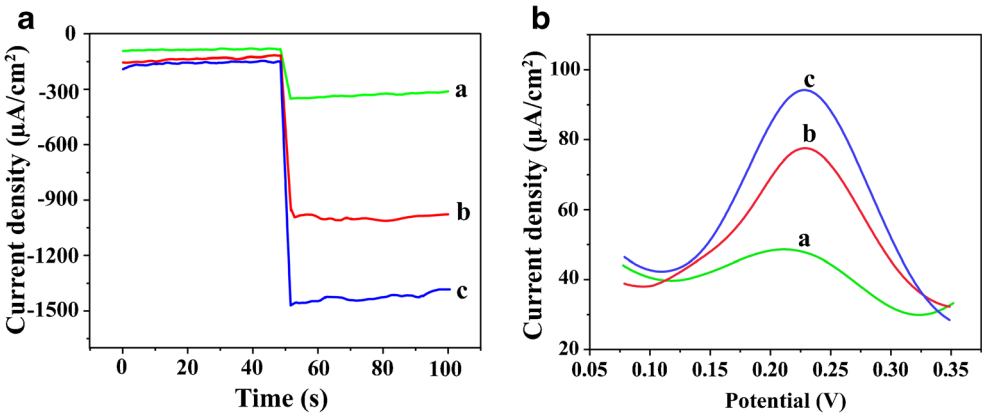

Fig. 4 I-t (**a**) and DPV (**b**) of the electrochemical biosensor with targets of different concentrations: (a) 0, (b) 1.5×10^5 CFU/mL, (c) 1.5×10^7 CFU/mL

determined by the combination degree of the Pt-Ni-Cu NCs and bacterial peptidoglycan. A series of duration times were set to detect the changes of the signal while other conditions remained unchanged. Figure S3a shows that the signal increased when the duration time was 20 to 80 min, and then decreased when the duration time was 80 to 100 min. Based on the characteristics of the peptidoglycan combined with Pt-Ni-Cu NCs, we speculated that the signal reduction was attributed to the degree of the Pt-Ni-Cu NCs falling into the peptidoglycan.

In addition, the pH of the peptidoglycan combined with Pt-Ni-Cu NCs also played an essential role in signal output. Therefore, the reaction buffers with different pH were applied in the electrochemical biosensor. The signal increased from pH 5.0 to pH 7.0 (Fig. S3b). When the pH of the buffer reached the weak alkaline condition (7.0→7.5), the signal obviously decreased. Hence, pH 7.0 was selected as the best pH reaction condition.

Finally, the concentrations of Pt-Ni-Cu NCs were optimized, which not only maximized the electrochemical signal intensity but significantly reduced the cost of the experiment. As shown in Fig. S3c, the signal significantly increased with a higher concentration of the Pt-Ni-Cu NCs. However, when the concentration was from 1.1 to 1.7 mg/mL, the signal went to the plateau stage instead of changing significantly. Therefore, considering the principle of high efficiency and economy, 1.7 mg/mL was selected as the optimum reaction concentration.

Quantitative measurement of the electrochemical biosensor

For determining the sensitivity of the electrochemical biosensor, the proportional relationship between bacterial concentration and electrochemical signal intensity was investigated. As mentioned above, i-t was chosen as the form of signal output in the linear analysis due to its high sensitivity among electrochemical methods, which could improve the overall signal intensity as well as increase the signal differences between concentration gradients. As shown in Fig. 5a, the i-t signals linearly increased when the bacteria concentration ranged from 1.5×10^2 CFU/mL to 1.5×10^8 CFU/mL in the working potential of − 0.4 V. Moreover, a strong linear correlation existed between the logarithm of concentration and i-t intensities. The linear equation was attained from linear relation ($I = 22.4–177\ \lg C_{S.aureus}$), where I was electrochemical intensity, and $C_{S.aureus}$ represented the concentration of *S. aureus* (Fig. 5b). In addition, the detection limit was calculated to be 42 CFU/mL depending on the blank detection value and the standard deviation. The reproducibility of the bacterial biosensor was verified using four electrodes to detect the concentration of 100 CFU/mL. The relative standard deviation (RSD) was 12%. Then, the same electrode was utilized to detect the reproducibility four times at the concentration of 100 CFU/mL, and the RSD was 8.8%. The analytical figures of other electrochemical bacterial detection methods (detection limit and linear range) were compared with this method (Table S1). The developed electrochemical biosensor was superior due to a wider linear range and lower detection limit for bacterial detection. In conclusion, the Pt-Ni-Cu NCs provided good linear relationship, sensitivity, and stability for the electrochemical biosensor, which was caused by its efficient catalysis and effective combination with bacteria.

The specificity of the electrochemical biosensor

Specificity was tested by detecting different serotypes of bacteria and different types of bacteria by the electrochemical biosensor. Firstly, two strains of non-*S. aureus* (*K. pn*, *E. coil*) and two strains of *S. aureus* (*S. au22923*, *S. au21293*) were chosen as the target bacteria. The bacterial concentration of 1.5×10^7 CFU/mL was chosen as the detection concentration in specificity detection. In Fig. 6a, the two serotypes of *S. aureus* achieved strong electrochemical intensities relative to other serotypes, which indicated that the antibody determined the specificity of the electrochemical biosensor. Furthermore, to confirm the general applicability of the electrochemical biosensor in Gram-positive bacteria, the

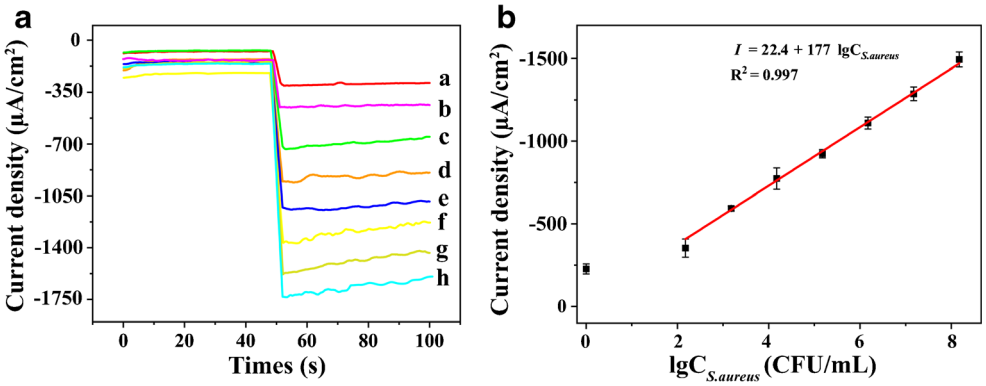

Fig. 5 (**a**) Electrochemical signal intensities of the proposed electrochemical biosensor under different concentrations of *S. aureus* (0 CFU/mL a, 1.5×10^2 CFU/mL b, 1.5×10^3 CFU/mL c, 1.5×10^4 CFU/mL d, 1.5×10^5 CFU/mL e, 1.5×10^6 CFU/mL f, 1.5×10^7 CFU/mL g, 1.5×10^8 CFU/mL h). (**b**) The linear correlation between the electrochemical signal intensities and the logarithm of *S. aureus* concentrations

antibody was replaced by the antibody of anti-*S. pn*. Similarly, as seen in Fig. 6b, the electrochemical intensity of *S. pn* was significantly higher than in other bacterial groups. According to these results, the electrochemical biosensor possessed high specificity and broad-spectrum detection capacity for Gram-positive bacteria due to the assistance of the antibody and the peptidoglycan.

Recovery test of the electrochemical biosensor

To evaluate the clinical application of the proposed electrochemical biosensor, the recovery experiments in biological samples were examined. Firstly, the common body fluids-urine samples were selected for the recovery test. The urine samples were diluted five times by 0.01 M PBs. Then, different concentrations of bacteria were added to the sample, which was thoroughly mixed before testing. As shown in Table S2, the relative standard deviations changed from 1.5 to 2.2%, and the recoveries were between 90.4 and 107% (three repetitions). The relatively low standard deviation and well recovery indicated that the electrochemical biosensor possessed a high potential to detect pathogenic microorganisms in complex clinical samples.

Challenges for electrochemical biosensor

In this work, we constructed a novel non-enzyme electrochemical biosensor for the rapid detection of Gram-positive bacteria by the combination between the peptidoglycan and Pt-Ni-Cu NCs. The proposed biosensor has achieved acceptable results in sensitivity and specificity analysis. However, there are still some self-limitation about the electrochemical biosensor, such as the unsatisfactory reversibility, storage lifetime, and complex samples detection ability of the biosensor. First, the regeneration solution may destruct the conductivity and stability of the C-CNTs [35], or existing difficulty in fully separating the antibody and bacteria which was a very large antigen. Second, the unsatisfactory storage lifetime probably resulted from the binding process of peptidoglycan and Pt-Ni-Cu NCs. As shown in Fig. S3a, the longtime combination made Pt-Ni-Cu NCs completely wrapped by peptidoglycan [33], blocking the signal output. Finally, in complex samples such as serum, the detection ability was still not satisfactory. It is very likely that the complex proteins and cell products will seriously impact on interface detection through the non-specific adsorption. Thus, in the following experiments, we will further improve the comprehensive performance of the

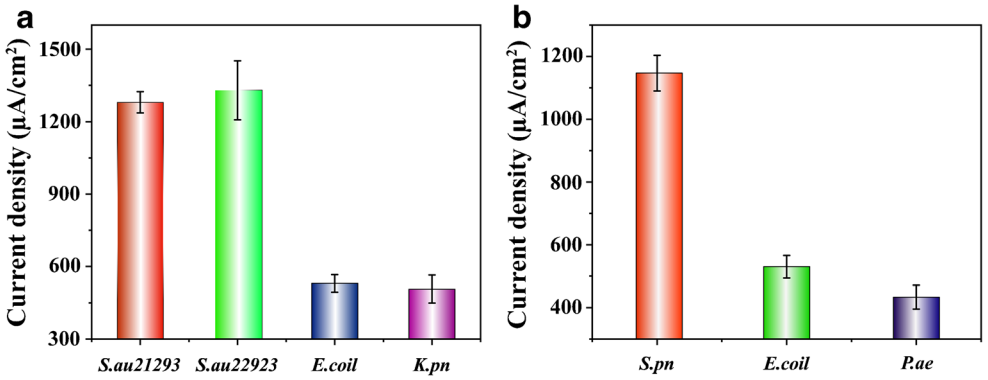

Fig. 6 **a** Specificity analysis of electrochemical biosensor by detecting different serotypes of *S. aureus* (*S. au21293*, *S. au22923*) and other types of bacteria (*K. pn*, *E. coli*). The bacterial concentration of the specificity analysis was 1.5×10^7 CFU/mL. **b** Specificity analysis of electrochemical biosensor by detecting *S. pn* and other types of bacteria (*E. coli*, *P. ae*). The bacterial concentration of the specificity analysis was 1.5×10^7 CFU/mL

biosensor through optimizing the interface modification and signal substance etc.

Conclusions

In this study, we presented a novel signal-enhanced non-enzyme electrochemical biosensor based on the highly efficient combination effect of the peptidoglycan and Pt-Ni-Cu NCs, for rapid detection of Gram-positive bacteria. In general, the electrochemical biosensor not only exploited the potential value of the peptidoglycan network of Gram-positive bacteria but also simultaneously made full use of the peroxidase-like activity and intrinsic electrochemical characteristic of Pt-Ni-Cu NCs. The proposed electrochemical biosensor was fast, with high specificity and wide linear range for Gram-positive bacteria detection, which might provide a potential alternative for clinical pathogenic bacteria detection and POCT.

Funding This study was financially supported by the National Natural Science Foundation of China (81873980, 81873972, 21804015), the National Science and Technology Major Project of the Ministry of Science and Technology of China (2018ZX10732202), and the Natural Science Foundation Project of CQ (cstc2018jcyjAX0201, cstc2018jcyjAX0251).

Compliance with ethical standards

Conflict of interest The authors declare no competing interests.

References

1. Al Tall Y, Abualhaijaa A, Alsaggar M, Almaaytah A, Masadeh M, Alzoubi KH (2019) Design and characterization of a new hybrid peptide from LL-37 and BMAP-27. Infect Drug Resist 12:1035–1045. https://doi.org/10.2147/IDR.S199473
2. Goad B, Harris LK (2018) Identification and prioritization of macrolideresistance genes with hypothetical annotation inStreptococcus pneumoniae. Bioinformation 14(9):488–498. https://doi.org/10.6026/97320630014488
3. Koirala B, Phillips NR, Tal-Gan Y (2019) Unveiling the importance of amide protons in CSP:ComD interactions in Streptococcus pneumoniae. ACS Med Chem Lett 10(6):880–886. https://doi.org/10.1021/acsmedchemlett.9b00038
4. Panda PS, Chaudhary U, Dube SK (2016) Comparison of four different methods for detection of biofilm formation by uropathogens. Indian J Pathol Microbiol 59(2):177–179. https://doi.org/10.4103/0377-4929.182013
5. Borghei Y, Hosseini M, Ganjali MR (2017) Fluorometric determination of microRNA via FRET between silver nanoclusters and CdTe quantum dots. Microchim Acta 184(12):4713–4721. https://doi.org/10.1007/s00604-017-2512-9
6. Zhao H, Shu G, Zhu J, Fu Y, Gu Z, Yang D (2019) Persistent luminescent metal-organic frameworks with long-lasting near infrared emission for tumor site activated imaging and drug delivery. Biomaterials 217:e119332. https://doi.org/10.1016/j.biomaterials.2019.119332
7. Han DB, Yan YR, Wang JM et al (2019) An enzyme-free electrochemiluminesce aptasensor for the rapid detection of Staphylococcus aureus by the quenching effect of MoS2-PtNPs-vancomycin to S2O82−/O2 system. Sensors Actuators B Chem 288:586–593. https://doi.org/10.1016/j.bios.2013.03.084
8. Zhang L, Deng H, Yuan R, Yuan Y (2019) Electrochemical lead(II) biosensor by using an ion-dependent split DNAzyme and a template-free DNA extension reaction for signal amplification. Microchim Acta 186(11). https://doi.org/10.1007/s00604-019-3857-z
9. Asif M, Haitao W, Shuang D, Aziz A, Zhang G, Xiao F, Liu H (2017) Metal oxide intercalated layered double hydroxide nanosphere: with enhanced electrocatalyic activity towards H2O2 for biological applications. Sensors Actuators B Chem 239:243–252. https://doi.org/10.1016/j.snb.2016.08.010
10. Guo B, Wen B, Cheng W, Zhou X, Duan X, Zhao M, Xia Q, Ding S (2018) An enzyme-free and label-free surface plasmon resonance biosensor for ultrasensitive detection of fusion gene based on DNA self-assembly hydrogel with streptavidin encapsulation. Biosens Bioelectron 112:120–126. https://doi.org/10.1016/j.bios.2018.04.027
11. Asif M, Aziz A, Azeem M, Wang Z, Ashraf G, Xiao F, Chen X, Liu H (2018) A review on electrochemical biosensing platform based on layered double hydroxides for small molecule biomarkers determination. Adv Colloid Interf Sci 262:21–38. https://doi.org/10.1016/j.cis.2018.11.001
12. Asif M, Liu H, Aziz A, Wang H, Wang Z, Ajmal M, Xiao F, Liu H (2017) Core-shell iron oxide-layered double hydroxide: high electrochemical sensing performance of H2O2 biomarker in live cancer cells with plasma therapeutics. Biosens Bioelectron 97:352–359. https://doi.org/10.1016/j.bios.2017.05.057
13. Luo C, Tang H, Cheng W, Yan L, Zhang D, Ju H, Ding S (2013) A sensitive electrochemical DNA biosensor for specific detection of Enterobacteriaceae bacteria by Exonuclease III-assisted signal amplification. Biosens Bioelectron 48:132–137. https://doi.org/10.1016/j.bios.2013.03.084
14. Maduraiveeran G, Sasidharan M, Ganesan V (2018) Electrochemical sensor and biosensor platforms based on advanced nanomaterials for biological and biomedical applications. Biosens Bioelectron 103:113–129. https://doi.org/10.1016/j.bios.2017.12.031
15. Xu L, Liu Z, Lei S, Huang D, Zou L, Ye B (2019) A sandwich-type electrochemical aptasensor for the carcinoembryonic antigen via biocatalytic precipitation amplification and by using gold nanoparticle composites. Microchim Acta 186(7):473. https://doi.org/10.1007/s00604-019-3542-2
16. Jiang HL, Ma X, Wang L, Zhang Q (2019) Switching on photocatalysis of metal-organic frameworks by engineering structural defects. Angew Chem Int Ed Eng 131:12303–12307. https://doi.org/10.1002/anie.201907074
17. Sun X, Tao Y, Du Y, Ding W, Chen C, Ma X (2019) Metal organic framework HKUST-1 modified with carboxymethyl-β-cyclodextrin for use in improved open tubular capillary electrochromatographic enantioseparation of five basic drugs. Microchim Acta 186(7):462–469. https://doi.org/10.1007/s00604-019-3584-5
18. Ohtani M, Muraoka T, Okimoto Y, Kobiro K (2017) Rapid one-pot solvothermal batch synthesis of porous nanocrystal assemblies composed of multiple transition-metal elements. Inorg Chem 56(19):11546–11551. https://doi.org/10.1021/acs.inorgchem.7b01192
19. Li W, Chen B, Zhang H, Sun Y, Wang J, Zhang J, Fu Y (2015) BSA-stabilized Pt nanozyme for peroxidase mimetics and its application on colorimetric detection of mercury(II) ions. Biosens Bioelectron 66:251–258. https://doi.org/10.1016/j.bios.2014.11.032

20. Xu X, Zhang X, Sun H, Yang Y, Dai X, Gao J, Li X, Zhang P, Wang HH, Yu NF, Sun SG (2014) Synthesis of Pt-Ni alloy nanocrystals with high-index facets and enhanced electrocatalytic properties. Angew Chem Int Ed Eng 53(46):12522–12527. https://doi.org/10.1002/anie.201406497
21. Mostafa S, Behafarid F, Croy JR, Ono LK, Li L, Yang JC, Frenkel AI, Cuenya BR (2010) Shape-dependent catalytic properties of Pt nanoparticles. J Am Chem Soc 132(44):15714–15719. https://doi.org/10.1021/ja106679z
22. Jin L, Meng Z, Zhang Y, Cai S, Zhang Z, Li C, Shang L, Shen Y (2017) Ultrasmall Pt nanoclusters as robust peroxidase mimics for colorimetric detection of glucose in human serum. ACS Appl Mater Interfaces 9(11):10027–10033. https://doi.org/10.1021/acsami.7b01616
23. Mu X, Wang J, Li Y, Xu F, Long W, Ouyang L, Liu H, Jing Y, Wang J, Dai H, Liu Q, Sun Y, Liu C, Zhang XD (2019) Redox trimetallic nanozyme with neutral environment preference for brain injury. ACS Nano 13(2):1870–1884. https://doi.org/10.1021/acsnano.8b08045
24. Asif M, Aziz A, Wang Z, Ashraf G, Wang J, Luo H, Chen X, Xiao F, Liu H (2019) Hierarchical CNTs@CuMn layered double hydroxide nanohybrid with enhanced electrochemical performance in H2S detection from live cells. Anal Chem 91(6):3912–3920. https://doi.org/10.1021/acs.analchem.8b04685
25. Pei F, Wang P, Ma E, Yu H, Gao C, Yin H, Li Y, Liu Q, Dong Y (2018) A sandwich-type amperometric immunosensor fabricated by Au@Pd NDs/Fe2+-CS/PPy NTs and Au NPs/NH2-GS to detect CEA sensitively via two detection methods. Biosens Bioelectron 122:231–238. https://doi.org/10.1016/j.bios.2018.09.065
26. Babamiri B, Bahari D, Salimi A (2019) Highly sensitive bioaffinity electrochemiluminescence sensors: recent advances and future directions. Biosens Bioelectron 142:111530. https://doi.org/10.1016/j.bios.2019.111530
27. Cabeen MT, Jacobs-Wagner C (2005) Bacterial cell shape. Nat Rev Microbiol 3(8):601–610. https://doi.org/10.1038/nrmicro1205
28. Johnson JW, Fisher JF, Mobashery S (2013) Bacterial cell-wall recycling. Ann N Y Acad Sci 1277:54–75. https://doi.org/10.1111/j.1749-6632.2012.06813.x
29. Wu R, Ma Y, Pan J, Lee SH, Pan G (2017) Efficient capture, rapid killing and ultrasensitive detection of bacteria by a nano-decorated multi-functional electrode sensor. Biosens Bioelectron 101:52–59. https://doi.org/10.1016/j.bios.2017.10.003
30. Kashyap DR, Wang M, Liu LH, Boons GJ, Gupta D, Dziarski R (2011) Peptidoglycan recognition proteins kill bacteria by activating protein-sensing two-component systems. Nat Med 17(6):676–683. https://doi.org/10.1038/nm.2357
31. Turner RD, Hurd AF, Cadby A, Hobbs JK, Foster SJ (2013) Cell wall elongation mode in Gram-negative bacteria is determined by peptidoglycan architecture. Nat Commun 4:1496–1503. https://doi.org/10.1038/ncomms2503
32. Girardin SE, Boneca IG, Carneiro LA et al (2003) Nod1 detects a unique muropeptide from gram-negative bacterial peptidoglycan. Science 300(5625):1584–1587. https://doi.org/10.1126/science.1084677
33. Fang G, Li W, Shen X, Perez-Aguilar JM, Chong Y, Gao X, Chai Z, Chen C, Ge C, Zhou R (2018) Differential Pd-nanocrystal facets demonstrate distinct antibacterial activity against Gram-positive and Gram-negative bacteria. Nat Commun 9(1):129–137. https://doi.org/10.1038/s41467-017-02502-3
34. Ye JS, Chen C, Lee C (2015) Pd nanocube as non-enzymatic glucose sensor. Sensors Actuators B Chem 208:569–574. https://doi.org/10.1016/j.snb.2014.11.091
35. Niroula J, Premaratne G, Ali Shojaee S, Lucca DA, Krishnan S (2016) Combined covalent and noncovalent carboxylation of carbon nanotubes for sensitivity enhancement of clinical immunosensors. Chem Commun (Camb) 52(88):13039–13042. https://doi.org/10.1039/c6cc07022a
36. Wu Y, Wang D, Chen X, Zhou G, Yu R, Li Y (2013) Defect-dominated shape recovery of nanocrystals: a new strategy for trimetallic catalysts. J Am Chem Soc 135(33):12220–12223. https://doi.org/10.1021/ja4068063
37. Feng X, Zhang Y, Zhou J, Li Y, Chen S, Zhang L, Ma Y, Wang L, Yan X (2015) Three-dimensional nitrogen-doped graphene as an ultrasensitive electrochemical sensor for the detection of dopamine. Nanoscale 7(6):2427–2432. https://doi.org/10.1039/c4nr06623e
38. Wei Y, Li X, Sun X, Ma H, Zhang Y, Wei Q (2017) Dual-responsive electrochemical immunosensor for prostate specific antigen detection based on Au-CoS/graphene and CeO2/ionic liquids doped with carboxymethyl chitosan complex. Biosens Bioelectron 94:141–147. https://doi.org/10.1016/j.bios.2017.03.001
39. Aziz A, Asif M, Azeem M, Ashraf G, Wang Z, Xiao F, Liu H (2019) Self-stacking of exfoliated charged nanosheets of LDHs and graphene as biosensor with real-time tracking of dopamine from live cells. Anal Chim Acta 1047:197–207. https://doi.org/10.1016/j.aca.2018.10.008
40. Asif M, Aziz A, Wang H, Wang Z, Wang W, Ajmal M, Xiao F, Chen X, Liu H (2019) Superlattice stacking by hybridizing layered double hydroxide nanosheets with layers of reduced graphene oxide for electrochemical simultaneous determination of dopamine, uric acid and ascorbic acid. Microchim Acta 186(2):61–71. https://doi.org/10.1007/s00604-018-3158-y